ANALELE UNIVERSITĂȚII
"EFTIMIE MURGU" REȘIȚA
ANUL XVII, NR. 1, 2010, ISSN 1453 - 7397

Cristian Rugină, Pier Paolo Delsanto, Veturia Chiroiu, Ligia Munteanu

The Predicting of the Size Effects in the Buckling of the Carbon Nanotubes

It is well-known that the nanoindentation hardness displays strong indentation size effects. In this paper, the size dependence of the hardness with respect to the depth and the indenter radius for the buckling of multiwalled carbon nanotubes is investigated using the Toupin-Mindlin strain gradient theory. As expected, the indentation hardness is closely related to the depth and the indenter radius. Qualitatively, the responses of the axially compressed multiple walled carbon nanotube agree remarkable well with the experimental observations.

Keywords: *Nanoindentation, carbon nanotubes, buckling, size effects, Toupin-Mindlin theory.*

1. Introduction

Indentation is a testing method which received considerable recent interest in the mechanical characterisation of materials [1]-[4]. The goal of such testing is to extract elastic modulus and hardness of the specimen material from readings of indenter load and depth of penetration.

The size dependence of the nanoindentation is an open problem. There are numerous indentation tests at scales on the order of a micron or a submicron which have shown that the hardness increases significantly with decreasing the indenter size [5]. This can be attributed to the evolution of the so-called geometrically necessary dislocations beneath the indenter, which gives rise to strain gradients. On the micron or nanometer scale, the size effect of the deformation is inherent [6, 7]. Similarly indentation on the nano/microscale also displays a strong size effect. For example, the spreading of intershell distances and the inlayer van der Waals interactions in carbon nanotubes depend on the size of the tube [8, 9]. The mechanical properties are size dependent with respect to different dimensions and geometries of the carbon nanotubes [10]-[12].

The necessity for higher-order continuum theories originates from the inability of the classical theories to account for observed the size effects on the micro and nanoscales [13, 14]. These effects usually manifest themselves as an increase in the strength with respect to decreasing the size of the structure when the length scale is of the order of microns.

The objective of this paper is to investigate the size dependence of the hardness with respect to the depth and the indenter radius for the shell buckling of multiwalled carbon nanotubes. The Toupin-Mindlin strain gradient theory is used to explain the size influence on the hardness, by taking account on the higher-order stress gradient contribution in the shear resistance of the neighboring walls during buckling of the multiwalled nanotubes.

2. Toupin-Mindlin theory

Let us consider the Toupin-Mindlin strain gradient theory in the rectangular coordinate system. We assume that the strain gradient tensor η_{ijk} and the double stress tensor τ_{ijk} with dimensions force per unit length, are present in the material body together with the conventional Eulerian strain tensor ε_{ij} and Cauchy stress tensor σ_{ij}. The components of the strain and strain gradient tensors are defined by

$$\varepsilon_{ij} = \frac{1}{2}(u_{i,j} + u_{j,i}),\ \eta_{ijk} = \varepsilon_{jk,i} = u_{k,ij} = \eta_{ikj},\ i, j, k = 1, 2, 3, \tag{1}$$

where u_i, $i = 1, 2, 3$ are displacements. ε_{ij} and η_{ijk} are symmetric with respect to the indices i and j, and accordingly, the Cauchy stress tensor σ_{ij} and the double stress tensor τ_{ijk} are also symmetric with respect to i and j. Consequently, under any small perturbations of the strains and strain gradients, $\delta\varepsilon_{ij}$ and $\delta\eta_{ijk}$, the work deviation may be obtained by the two pairs of work-conjugates

$$\delta W = \sigma_{ij}\delta\varepsilon_{ij} + \tau_{ijk}\delta\eta_{ijk}.$$

In addition, within the framework of linear elasticity, the following generalized Hooke's law between σ_{ij} and ε_{ij}, and τ_{ijk} and η_{ijk}, respectively, is assumed

$$\begin{aligned} \sigma_{ij} &= \lambda\varepsilon_{kk}\delta_{ij} + 2\mu\varepsilon_{ij}, \\ \tau_{ijk} &= \xi_1 l^2(\eta_{ipp}\delta_{jk} + \eta_{jpp}\delta_{ik}) + \xi_2 l^2(\eta_{ppi}\delta_{jk} + 2\eta_{kpp}\delta_{ij} + \eta_{ppj}\delta_{ik}) + \\ &+ \xi_3 l^2\eta_{ppk}\delta_{ij} + \xi_4 l^2\eta_{ijk} + \xi_5 l^2(\eta_{kji} + \eta_{kij}), \end{aligned} \tag{2}$$

where λ and μ are the conventional Lamé constants, ξ_i, $i=1,2,...,5$, are the elastic constants associated with the gradient terms, while l denotes an internal length scale resulted by the introduction of the strain gradients. It is related to the dimension of microstructure in the material. The positive definiteness of the strain energy density requires

$$\mu>0,\ 3\lambda+2\mu>0,\ \overline{\xi}_2>0,\ 5\overline{\xi}_1+2\overline{\xi}_2>0,$$
$$-\overline{d}_1<\overline{d}_2<\overline{d}_1,\ 5\overline{f}^2<6(\overline{d}_1-\overline{d}_2)(5\overline{\xi}_1+2\overline{\xi}_2),$$
$$18\overline{d}_1=-2\xi_1+4\xi_2+\xi_3+6\xi_4-3\xi_5,$$
$$18\overline{d}_2=2\xi_1-4\xi_2-\xi_3,\ \ 3\overline{\xi}_1=2(\xi_1+\xi_2+\xi_3),$$
$$\overline{\xi}_2=\xi_4+\xi_5,\ 3\overline{f}=\xi_1+4\xi_2-2\xi_3.$$

In the absence of body and inertia forces, the equilibrium equations written in terms of Cauchy stress σ_{ij} and the higher-order stress τ_{ijk} are

$$\sigma_{ik,i}-\tau_{ijk,ji}=0. \tag{3}$$

Substituting (1) and (2) into (3), the equilibrium equations can be written with respect to displacements

$$\begin{aligned}&\lambda u_{p,pi}\delta_{ik}+\mu(u_{i,ki}+u_{k,ii})-\xi_1 l^2(u_{p,ipji}\delta_{jk}+u_{p,jpji}\delta_{ik})-\\&-\xi_2 l^2(u_{i,ppji}\delta_{jk}+2u_{p,kpji}\delta_{ij}+u_{j,ppji}\delta_{ik})-\xi_3 l^2 u_{k,ppji}\delta_{ij}-\\&-\xi_4 l^2 u_{k,ijji}-\xi_5 l^2(u_{i,kjji}+u_{j,kiji})=0,\end{aligned} \tag{4}$$

To write the boundary conditions, the external surface S may be divided into two parts: the surface boundary S_σ for static forces, and the surface boundary S_u for displacements. On S_σ, the boundary conditions read as

$$T_k=n_i(\sigma_{ik}-\partial_j\tau_{ijk}),\ R_k=n_i n_j\tau_{ijk},$$

where T_k and R_k are the surface tractions and higher-order surface tractions, respectively. The above boundary conditions represent the conventional traction and higher-order traction conditions for a gradient-dependent material body. In the following we suppose that the contribution of τ_{ijk} is zero. So, T_k and R_k become

$$T_k=n_i\sigma_{ik},\ R_k=0. \tag{5}$$

On S_u the boundary conditions are given by

$$u_k=\overline{u}_k,\ n_l\partial_l u_k=\overline{e}_k, \tag{6}$$

where $\overline{u}_k$ denotes the known displacements and $\overline{e}_k$ represent the known normal gradient of $\overline{u}_k$.

3. Results for the spherical nanoindentation

In the literature it has been shown that for a spherical indentation in a homogeneous material, the indentation size effect depends on the indenter radius rather than penetration depth. In order to investigate these effects, we carried our analyses of indentation with indenters of different radii, as well as different penetration depth [15].

The comparison of our simulations against experiments is not the focus of the present paper. Our intention is to explain via Toupin-Mindlin theory the well-known size effect regarding hardness versus depth and hardness versus indenter radius in nanoindentation experiments. Therefore, we will discuss the results with experimental results if available or earlier similar results obtained by theories different from that presented here [10].

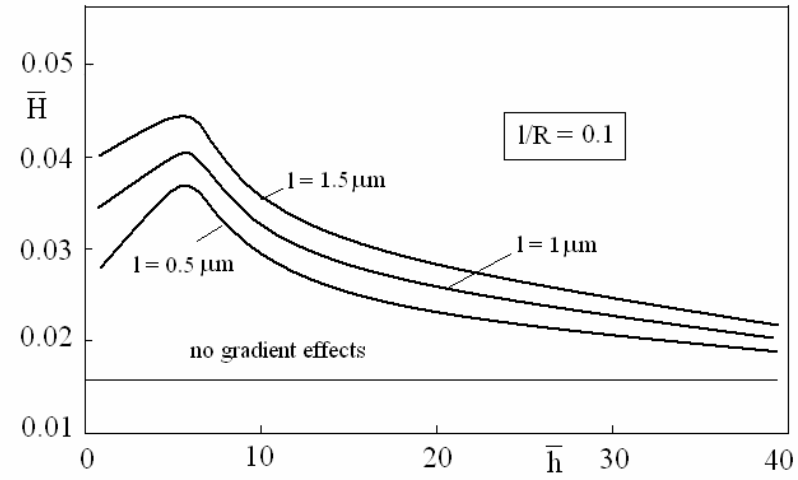

Figure 1. The hardness versus various indentation depths in the case $l/R = 0.1$.

Let us consider the following values of the material parameters $\lambda = 1.42\text{TPa}$, $\mu = 2.31\text{TPa}$, $\xi_1 = 0.5\,\text{TPa}\cdot\text{m}^{-2}$, $\xi_j = 0.1\,\text{TPa}\cdot\text{m}^{-2}$, $j = 2,...,5$. We consider three values for l = 0.5, 1 and $1.5\,\mu\text{m}$, and $l/R = 0.1$, 0.04 and 0.008, where l denotes an internal length scale which appears in (4). These cases corresponds to the

indenter radii $R = 5$, 10 and $15\,\mu\text{m}$, $R = 12.5$, 25 and $37.5\,\mu\text{m}$, and $R = 62.5$, 125 and $187.5\,\mu\text{m}$, respectively.

Figure 1 presents the dimensionless hardness ($\bar{H} = H / H_0$) with $H_0 = 1\text{TPa}$, versus the dimensionless indentation depth ($\bar{h} = h / h_0$) with $h_0 = 1\text{nm}$, for $l / R = 0.1$. The baseline corresponds to no gradient effects. The hardness $\bar{H}$ increases up to $\bar{h} = 8$ (corresponding to $P = 2.18\,\mu\text{m}$) and after that we observe a falling hardness with respect to increasing indentation depth ($\bar{h} > 8$), above the baseline case with no gradient effects. The effect is weaker for smaller indenter radii.

The profile of the curve presented in figure 1 is similar to those obtained in [16], by applying a theory of strain-gradient viscoplasticity with finite deformations for isotropic materials. Another model with a similar profile of the curve is based on a micromechanical model that assesses a nonlinear coupling between the statistically stored dislocations and the geometrically necessary dislocations [5]. While our theory of nanoindentation remains in the elastic range, the aforementioned theories' attempt is to capture the micro and nano-indentation size effect via the dependency on plastic strain gradients.

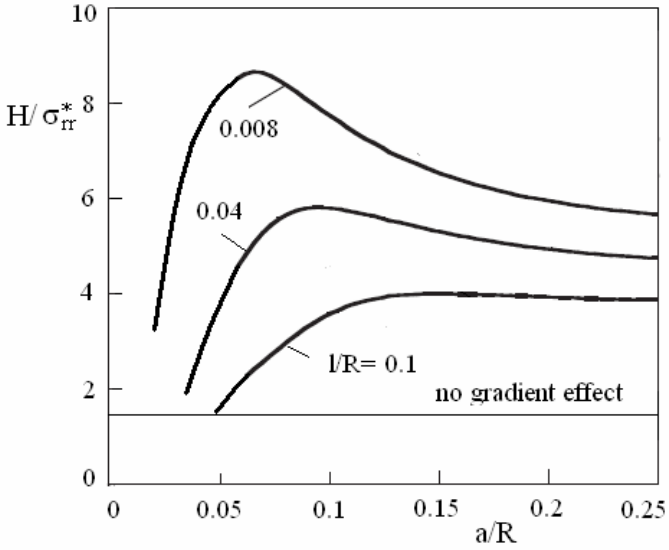

Figure 2. Ratios between the hardness H and σ_{rr}^{*} as functions of a / R.

Plots of the ratios of the hardness H and the generalized stress components σ^*_{rr}, $\sigma^*_{r\varphi}$ and $\sigma^*_{r\theta}$, respectively as functions of a/R and $l/R = 0.1$, 0.04 and 0.008, are presented in figures 2-4.

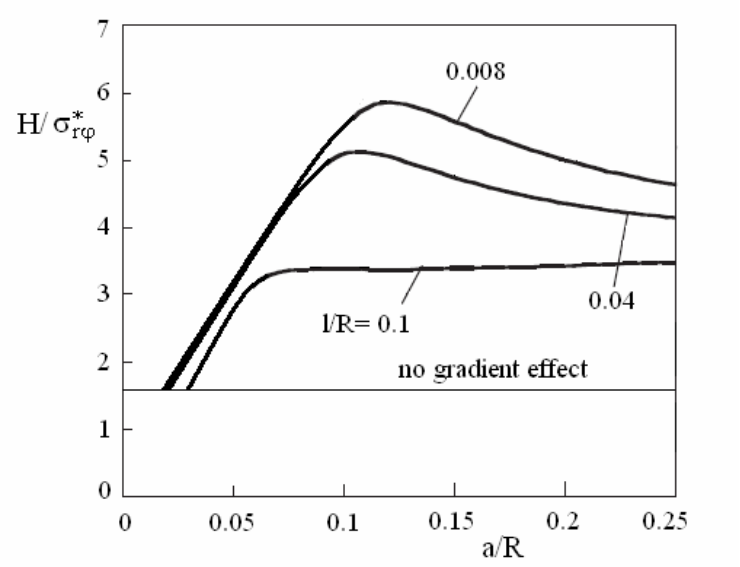

Figure 3. Ratios between the hardness H and $\sigma^*_{r\varphi}$ as functions of a/R.

Figure 5 presents the dimensionless hardness $\bar{H}$ with $H_0 = 1\text{TPa}$, versus the dimensionless indentation depth ($\bar{h} = h/h_0$) with $h_0 = 1\text{nm}$, for $l/R = 0.008$. The baseline corresponds to no gradient effects. The hardness $\bar{H}$ gradually slows up for $\bar{h} \le 8$ and rapidly increases with respect to increasing $8 < \bar{h} < 30$. For $\bar{h} > 30$, the increase in $\bar{H}$ becomes less sensitive to $\bar{h}$. This type of behavior is similar to those obtained in [15].

The Toupin-Mindlin theory is evaluated in order to predict and explain this peculiar behavior. The decrease or increase in $\bar{H}$ is believed to be closely associated with the loading P and the inner walls size in multiwalled nanotubes.

When the dimensions of the indenter radius are comparable to the intershell walls size (figure 1), the indenter motion is easier for $P > 2.18\,\mu\text{m}$, and difficult for $P < 2.18\,\mu\text{m}$. In the first case, the hardness is decreasing with respect to the indentation depth, while in the second case, the effect is reversed.

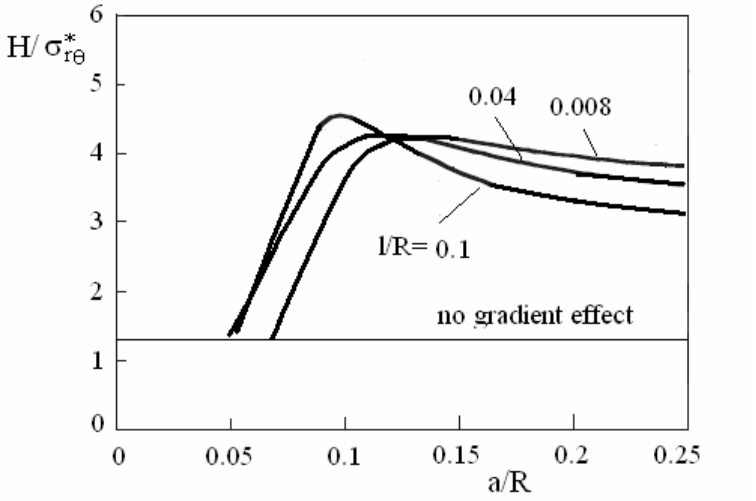

Figure 4. Ratios between the hardness H and $\sigma_{r\theta}^{*}$ as functions of a/R.

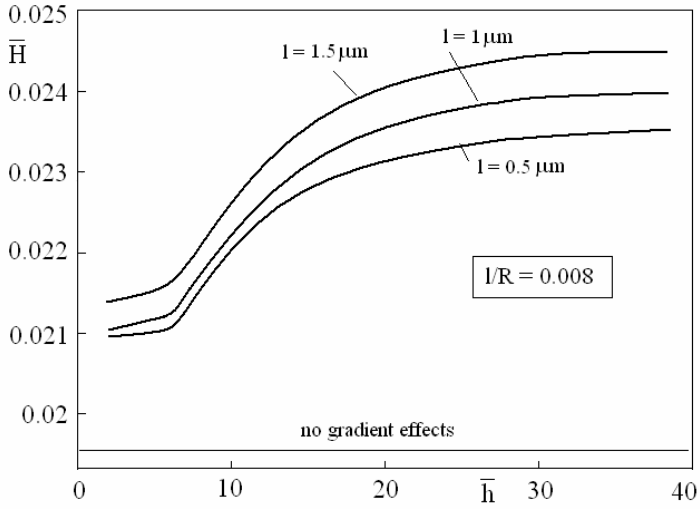

Figure 5. The hardness versus indentation depth in the case $l/R = 0.008$.

When the dimensions of the indenter radius are larger than the intershell size (figure 5), the walls are impenetrable and the indenter motion is difficult. This

leads to a strain hardening of the material, and the hardness is increasing with respect to the indentation depth. For $P < 2.18\,\mu m$ the increase is slowly but becomes rapidly for $P > 2.18\,\mu m$.

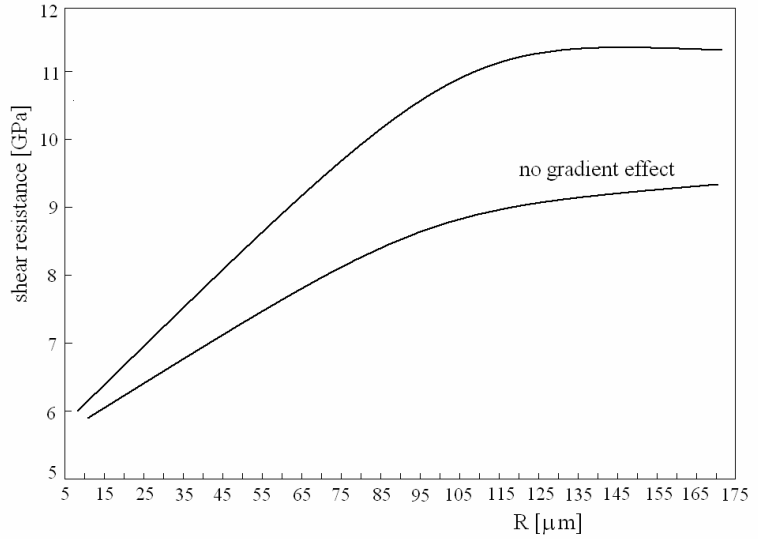

Figure 6. Shear resistance between the neighboring walls of the multiwalled nanotubes.

By comparing figures 1 and 5, we see that the hardness increases significantly with respect to decreasing of the indenter size. For $P > 2.18\,\mu m$, the intershell of the nanotubes come into contact with the indenter tip and the increase in load has different actions depending on the indenter size.

The indenter penetrability into material depends on the shear resistance of the intershell walls during the buckling of the multiwalled nanotubes. The shear resistance is calculated by taking into account the higher-order stresses gradient contribution, the latter is plotted in figure 6. The value of the shear resistance is smaller for indenter radii $5\mu m \le R \le 15\mu m$ than for larger indenter radii $62.5\mu m \le R \le 187.5\mu m$. The resistance keeps a constant value for $R > 120$.

This can explain the tendency of the hardness to decrease with respect to the indentation depth for lower shear resistance, and to increase for larger shear resistance [10]. However, it should be noted that the higher-order stresses τ_{ijk} play an important role in refining the elastic buckling theory that account for additional physics. The results presented in this study show that the size significantly affects the nanoindentation hardness.

4. Conclusions

Conventional continuum theories are unable to capture the observed indentation size effects, due to the lack of intrinsic length scales that represent the measures of nanostructure in the constitutive relations. In order to overcome this deficiency, the Toupin-Mindlin strain gradient theory of nanoindentation is formulated in this paper and the size dependence of the hardness with respect to the depth and the radius of the indenter for multiple walled carbon nanotubes is investigated.

ACKNOWLEDGEMENTS: The authors gratefully acknowledge the financial support of the National Authority for Scientific Research (ANCS, UEFISCSU), Romania, through PN-II research project no. 106/2007, code ID_247/2007.

References

[1] Oliver, W.C., Pharr, G.M., *Improved technique for determining hardness and elastic modulus using load and displacement sensing indentation experiments*, Journal of Materials Research, 7(6), 1564–1580, 1992.
[2] Johnson, K.L., *Contact mechanics,* Cambridge University Press, New York, 1985.
[3] Dumitriu, D., Chiroiu,V., *On the dual equations in contact elasticity,* Rev. Roum. Sci,. Techn., serie Mécanique Appl., 51(3), 261–272, 2006.
[4] Dumitriu, D., Gauchs, G., Chiroiu, V., *Optimisation procedure for parameter identification in inelastic material indentation testing*, Rev. Roum. Sci. Techn., serie Mécanique Appl., 53(1), 43–54, 2008.
[5] Abu Al-Rub, R.K., *Predictionn of micro- and nano indentation size effect from conical or pyramidal indentation*, Mechanics of materials, 39(8), 787-802, 2007.
[6] Hutchinson, J.W., *Plasticity at the micron scale*, Int J Solids Structures, 37, 225–238, 2000.
[7] Evans, A.G., Hutchinson, J.W., *A critical assessment of theories of strain gradient plasticity*, Acta Materialia, 57, 1675–1688, 2009.
[8] Brenner, D. W., Shenderova, O. A., Areshkin, D. A., Schall, J. D., Frankland, S.J.V., *Atomic modeling of carbon-based nanostructures as a tool for developing new materials and technologies*, CMES: Computer Modeling in Engineering & Science, 3(5), 643–673, 2002.
[9] Srivastava, D., Atluri, S.N., *Computational Nano-technology: A Current Perspective*, CMES: Computer Modeling in Engineering & Sciences 3(5), 531–538, 2002.

[10] Chiroiu, V., Munteanu, L., Delsanto, P.P., *Evaluation of the Toupin-Mindlin Theory for Predicting the Size Effects in the Buckling of the Carbon Nanotubes*, CMC: Computers, Materials, & Continua, vol.453, 1-26, 2010.
[11] Chiroiu, V. , Munteanu. L. , Donescu, St., *On the mechanical modeling of single-walled carbon nanotubes*, Rev. Roum. Sci,. Techn., serie Mécanique Appl., 51(1), 37–52, 2006.
[12] Munteanu, L., Chiroiu, V., *Shell Buckling of Carbon Nanotubes Using Nanoindentation*, CMES: Computer Modeling in Engineering & Science, 48(1), 27–41, 2009.
[13] Toupin, R.A., *Elastic materials with couple stresses*. Arch. Ration. Mech. Anal. 11, 385–414, 1962.
[14] Mindlin, R.D., *Micro-structure in linear elasticity*. Arch. Ration. Mech. Anal. 16, 51–78, 1964.
[15] Ouyang, C., Li, Z., Huang, M., Hou, C., *Discrete dislocation analyses of virvular nanoindenttaion and its size dependence in polycrystals*, Acta Materialia 56**,** 2706-2717, 2008.
[16] Lele, S.P., Anand, L**.,** *A large-deformation strain-gradient theory for isotropic viscoplastic materials*, International Journal of Plasticity, 25, 420–453, 2009.

Addresses:

- Dr. Eng. Cristian Rugină, scientific researcher, Institute of Solid Mechanics of Romanian Academy, Ctin Mille 15, Bucharest 010141, e-mail: rugina.cristian@gmail.com, phone: 021 3153810.
- Prof. Dr. Pier Paolo Delsanto, Politecnico di Torino, Dip. Di Fisica, e-mail: pier.delsanto@polito.it, phone: +39 011 564 7311.
- Dr. Veturia Chiroiu, senior scientific researcher, Institute of Solid Mechanics of Romanian Academy, Ctin Mille 15, Bucharest 010141, e-mail: veturiachiroiu@hotmail.com, phone: 021 3153810.
- Dr. Ligia Munteanu, senior scientific researcher, Institute of Solid Mechanics of Romanian Academy, Ctin Mille 15, Bucharest 010141, e-mail: ligia_munteanu@hotmail.com, phone: 021 3153810.